

Dynamics of Catalytic Resolution of 2-Lithio-*N*-Boc-piperidine by Ligand Exchange

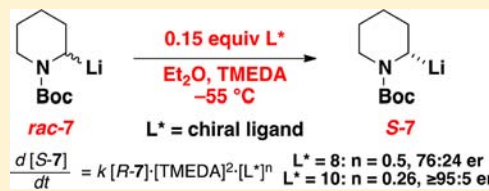
Timothy K. Beng,[†] William S. Tyree,[†] Trent Parker,[†] Chicheung Su,[‡] Paul G. Williard,[‡] and Robert E. Gawley^{*†}

[†]Department of Chemistry and Biochemistry, University of Arkansas, Fayetteville, Arkansas 72701, United States

[‡]Department of Chemistry, Brown University, Providence, Rhode Island 02912, United States

Supporting Information

ABSTRACT: The dynamics of the racemization and catalytic and stoichiometric dynamic resolution of 2-lithio-*N*-Boc-piperidine (**7**) have been investigated. The kinetic order in tetramethylethylenediamine (TMEDA) for both racemization and resolution of the title compound and the kinetic orders in two resolving ligands have been determined. The catalytic dynamic resolution is second order in TMEDA and 0.5 and 0.265 order in chiral ligands **8** and **10**, respectively. The X-ray crystal structure of ligand **10** shows it to be an octamer. Dynamic NMR studies of the resolution process were carried out. Some of the requirements for a successful catalytic dynamic resolution by ligand exchange have been identified.

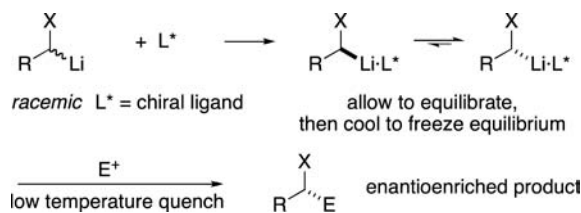


INTRODUCTION

Organolithium compounds are widespread in organic synthesis.¹ The use of stoichiometric chiral ligands such as (–)-sparteine complexed to *sec*-BuLi to effect enantioselective deprotonation represents one of the methods to generate scalemic organolithium compounds for use in asymmetric synthesis.² Unfortunately, effecting an asymmetric deprotonation on *N*-Boc-piperidines through the use of the chiral ligand (–)-sparteine is not as successful as with pyrrolidines,³ but partial success [enantiomeric ratio (er) of up to 88:12 in reasonable yields] has been achieved with O'Brien's diamine.⁴

In an important development, several chiral organolithium compounds that are amenable to dynamic thermodynamic resolution (DTR) have been discovered (Scheme 1).⁵ In DTR,

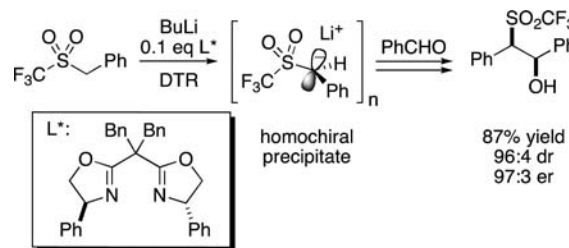
Scheme 1. Dynamic Thermodynamic Resolution (DTR) Using a Stoichiometric Amount of the Chiral Ligand L*



a racemic organolithium is generated, and a chiral ligand, L*, that can resolve the organolithium dynamically (an asymmetric transformation of the first kind) is then added. Dynamic resolutions hold significant potential, since they obviate the need for an enantioselective deprotonation or an asymmetric synthesis of an entioenriched precursor stannane. A disadvantage of DTR can arise if the electrophile used to react with the organolithium is also reactive toward, and

consumes L*. Thus, a variation of dynamic resolution using a catalytic amount of L* is desirable. Toru and co-workers reported a catalytic dynamic resolution (CDR) that is driven by the well-known phenomenon of crystallization-induced asymmetric transformation (Scheme 2).⁶ In the Toru example, the

Scheme 2. Toru's Catalytic Dynamic Resolution (CDR)

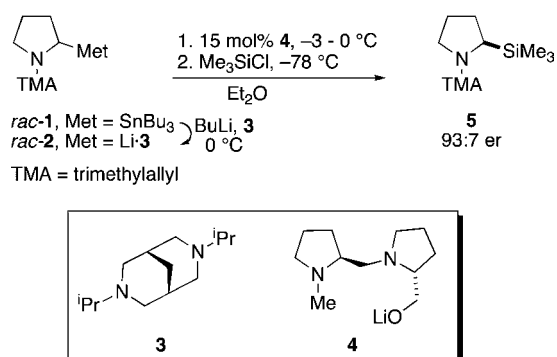


resolution is accomplished through dynamic resolution of planar-chiral organolithium enantiomers by the bisoxazoline ligand followed by precipitation of homochiral aggregates (an asymmetric transformation of the second kind). Addition of aldehyde caused dissolution of the precipitate, and after the reaction was quenched with Me₃SiCl and acidic workup, the product was isolated in good yield with excellent diastereoselectivity and enantioselectivity.

In 2009, we reported the transmetalation of 2-tributylstannyl-*N*-(trimethylallyl)pyrrolidine (**1**) in the presence of *N,N*-diisopropylbispidine (**3**) to afford racemic organolithium **2** (Scheme 3).⁷ Addition of ligand **4** (15 mol %) and stirring at ~0 °C effected a catalytic resolution. Cooling to –78 °C and

Received: August 6, 2012

Published: September 11, 2012

Scheme 3. CDR of 2-Lithio-*N*-(trimethylallyl)pyrrolidine (2)⁹

quenching with Me_3SiCl gave pyrrolidine **5** with an er of 93:7 (R:S).^{8,9}

In this catalytic resolution, organolithium **2** is in excess relative to the chiral resolving ligand **4**. The remaining **2** is presumably complexed to the achiral ligand **3**.¹⁰ To achieve a catalytic resolution, at a minimum it is necessary to ensure that the racemization of the organolithium is significantly slower than the dynamic resolution. Therefore, we studied the enantiomerization of **2** in the presence of the achiral bispidine ligand **3**,⁹ and the thermodynamic parameters were determined ($\Delta H^\ddagger = 25.1 \pm 1.4$ kcal/mol; $\Delta S^\ddagger = 8.1 \pm 5.0$ cal mol⁻¹ K⁻¹). Similarly, the thermodynamic parameters for the resolution of **2** by stoichiometric quantities of **4** in the presence of **3** were measured ($\Delta H^\ddagger = 25.1 \pm 1.7$ kcal/mol; $\Delta S^\ddagger = 14.2 \pm 6.1$ cal mol⁻¹ K⁻¹).¹¹ From these data, plots of ΔG^\ddagger versus temperature¹² revealed that the resolution of **2** by **4** has a lower barrier than enantiomerization at all temperatures between -80 and $+20$ °C.⁹

It should be noted that the catalytic resolution in Scheme 3 should not be called a dynamic *thermodynamic* resolution because it does not employ stoichiometric amounts of the chiral ligand.^{5g,13} Neither can it be called a dynamic *kinetic* resolution, as that term applies to systems where the organolithium inverts rapidly and the resolution occurs by asymmetric substitution under Curtin–Hammett conditions. Thus, we refer to the process simply as a catalytic dynamic resolution.

We wanted to know whether a CDR was possible in the absence of the achiral ligand, but since conversion of stannane **1** to organolithium **2** by tin–lithium exchange is not possible in the absence of the achiral ligand, we tested the possibility by extrapolation using varying amounts of bispidine **3**. Figure 1 shows the fraction of the *R* enantiomer of **5** as a function of the number of equivalents of bispidine **3** after treatment of *rac*-**2** with 15 mol % **4** for 1 h at 0 °C.⁹ The *y* intercept of 0.55

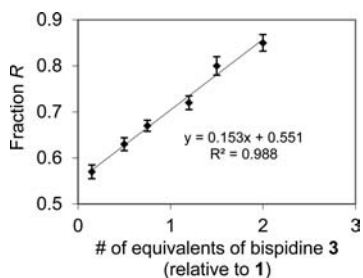
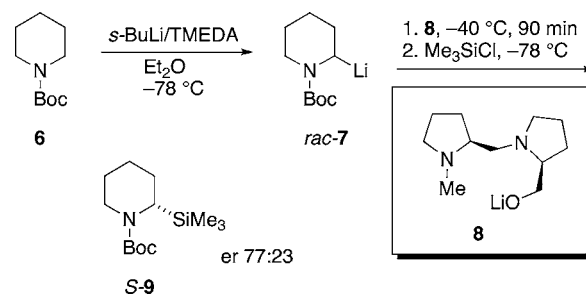


Figure 1. Resolution of **2** by **4** with varying amounts of bispidine **3** (0 °C, 1 h).⁹

implies that the er in the absence of **3** would be 55:45. The catalytic resolution of **2** by **4** is accelerated by **3**, but it is also apparent that **3** is necessary to achieve a CDR. If 15% of **2** is resolved to 93:7 er and the remaining 85% is racemic, the er of the solution would be 56:44, the same as the *y* intercept within experimental error. Therefore, a second requirement is that the chiral and achiral ligands must both be involved in the catalytic resolution. This could involve a total ligand exchange or a reorganization of the coordination of the organolithium to more than one ligand. Aggregation/deaggregation of the organolithium could be involved in the catalytic resolution by ligand exchange. Although the aggregation state of **2** was not determined, the aggregation state of the *N*-methyl analogue is a homochiral dimer, and the *N*-ethyl analogue is a mixture of aggregates.¹⁴

The mechanistic details of a catalytic resolution by ligand exchange are of interest. Unfortunately, a detailed mechanistic investigation of lithiopyrrolidine **2** is hampered by the fragility of the trimethylallyl group under the conditions of the reaction (it has a tendency to rearrange, undergo proton transfer, and be lost during workup). Also, the presence of the achiral bispidine ligand **3**¹⁵ complicates product purification and recovery of the conjugate acid of catalyst **4**.

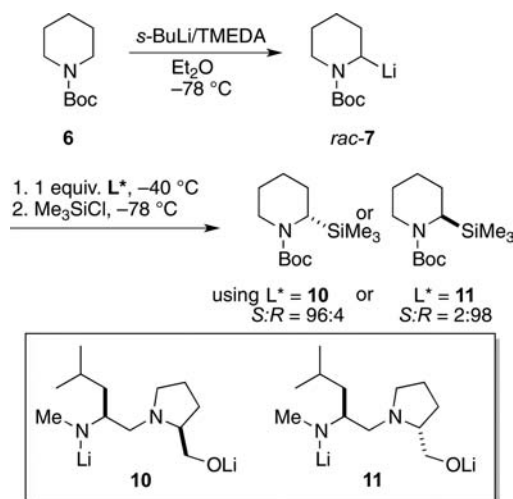
We wondered whether catalytic resolution involving ligand exchange is unique to the *N*-(trimethylallyl)pyrrolidine system in Scheme 3 or if other systems that can be resolved catalytically could be identified. As noted above, we believe that the free energy barrier for resolution must be lower than the free energy barrier for racemization. We therefore sought another system to investigate, and we chose 2-lithio-*N*-Boc-piperidine (**7**), which was shown by the Coldham group^{5f} to undergo stoichiometric resolution in the presence of tetramethylethylenediamine (TMEDA) (Scheme 4) and whose inversion dynamics were investigated jointly by our two groups.¹⁶

Scheme 4. DTR of **7**^{5f}

In lithiopiperidine **7**, we have an organolithium that is synthetically important and readily available. Moreover, the achiral ligand, TMEDA, is inexpensive. As it turned out (see Figure 14, below), the moderate final er of the Coldham resolution (77:23) permitted a crucial experiment that was not possible in investigating the more highly enantioselective catalytic resolution of **2**. An interesting fact uncovered previously was that both the stoichiometric resolution and the racemization of lithiopiperidine **7** are catalytic and first order in the *achiral* ligand TMEDA (0–2 equiv of TMEDA for the DTR and 0.1–1.0 equiv for the racemization). Also, several other diamine ligands were tested, and all of them failed to fill this catalytic role in the resolution—even tetraethylethylenediamine (TEEDA)!¹⁶

Herein we report the results of our detailed investigation into the dynamics of the catalytic resolution of **7** by **8**. During the course of this mechanistic investigation, we discovered a new pair of ligands, **10** and **11**, that effect the resolution of **7** and afford much higher enantioselectivity than **8** (Scheme 5).¹⁷ While many of these mechanistic studies were conducted with ligand **8**, we report some experiments with ligand **10** that provide additional insight into the processes involved.

Scheme 5. DTR of **7** with Ligands **10** and **11**^{17a}



RESULTS AND DISCUSSION

We previously reported the thermodynamic parameters for the racemization and resolution of **7**.¹⁶ The stoichiometric DTR of *rac*-**7** by **8** in the presence of 2 equiv of TMEDA has a large negative entropy of activation ($\Delta S^\ddagger = -55.9 \pm 1.8 \text{ cal mol}^{-1} \text{ K}^{-1}$) and a small enthalpy of activation ($\Delta H^\ddagger = 4.3 \pm 0.5 \text{ kcal/mol}$). The enantiomerization of **7** in the presence of 1 equiv of TMEDA has $\Delta H^\ddagger = 18.1 \pm 0.7 \text{ kcal/mol}$ and $\Delta S^\ddagger = 5.0 \pm 3.2 \text{ cal mol}^{-1} \text{ K}^{-1}$. At $-46 \text{ }^\circ\text{C}$, the free energy barriers for enantiomerization (in the presence of 2 equiv of TMEDA) and DTR (in the presence of 1 equiv of TMEDA) are equal. Below this temperature, the free energy barrier for DTR is lower. Given this information, we tested the possibility of a CDR of **7** at $-55 \text{ }^\circ\text{C}$ in the presence of TMEDA. The time evolution of the CDR of *rac*-**7** was evaluated as illustrated in Figure 2. In oven-dried vials, stannane *rac*-**12** was treated with BuLi and 1.2 equiv of TMEDA at $-78 \text{ }^\circ\text{C}$ for 1 h to effect tin–lithium exchange, affording *rac*-**7**·TMEDA. Chiral ligand **8** (15 mol %) was then added, and the reaction vessel was transferred to a thermostatted bath at an internal temperature of $-55 \text{ }^\circ\text{C}$. At various time intervals over 24 h, a vial was cooled to $-78 \text{ }^\circ\text{C}$ and quenched with Me_3SiCl , and the er was then measured by chiral-stationary-phase gas chromatography. The final er of the product (**77:23**) was the same as that obtained by Coldham et al.^{5f} using ligand **8** in a stoichiometric DTR; their experiment was duplicated in our hands as a control experiment. During the course of this experiment, no precipitate was observed in the reaction flask (compare with Scheme 2).

These data are noteworthy for two reasons. First, a CDR is operative, and second, the *S* organolithium is configurationally stable for at least 12 h under the reaction conditions, implying the achievement of an equilibrium state. During the course of this mechanistic investigation, the CDR using ligands **10** and **11**

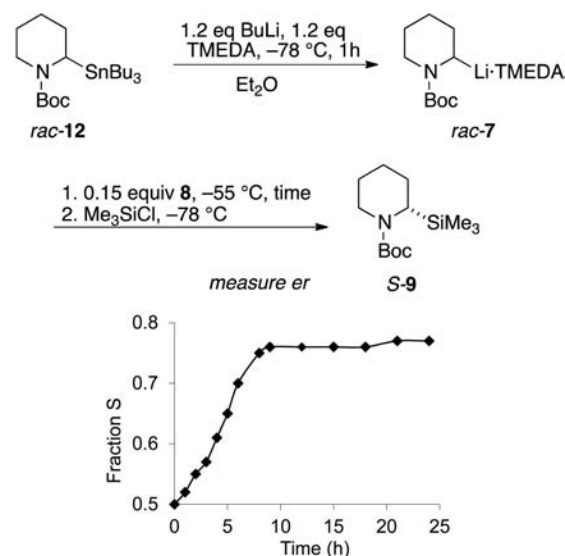


Figure 2. CDR of *rac*-**7** by **8**.

was found to be very highly enantioselective, and synthetic applications have been reported.¹⁷

Further investigations of the structure of lithiopiperidine **7** and the dynamics of enantiomerization, DTR, and CDR of **7** by **8** and **10** were undertaken at carefully controlled temperatures. These experiments, which are described in detail below, revealed the following:

- Conclusive evidence for the solution structure of **7** could not be obtained because the spectra are consistent with several possibilities, but evidence of dynamic exchange phenomena was found.
- There is variable configurational stability of **7** in the presence of different ligands at low temperature when **7** is generated by tin–lithium exchange.
- Although up to 1 equiv of TMEDA catalyzes the racemization and DTR of **7**,^{16,17} TMEDA retards racemization when present in excess; thus, excess TMEDA increases the configurational stability of **7**.
- There is a second-order dependence of the CDR on [TMEDA].
- The CDR has a fractional-order dependence on the concentration of the chiral ligand (**8** or **10**).

NMR Studies. Before describing the dynamics of lithiopiperidine **7**, we begin with the results of our study of its solution structure. It is known from in situ IR studies that the lithium ion of **7** is coordinated to the carbonyl oxygen, and the monomer structure in Figure 3 was proposed to be the structure in solution.^{4a} However, there are dimeric and polymeric structures that are consistent with the IR data. We used ^6Li and ^{13}C NMR spectroscopy to investigate the possible structures illustrated in Figure 3.

Transmetalation of stannanes *rac*-**12** and *S*-**12** with *n*-Bu⁶Li in ether/TMEDA provided $\{^6\text{Li}\}$ -**7**. The ^6Li and ^{13}C spectra were recorded at temperatures ranging from -80 to $-30 \text{ }^\circ\text{C}$. The ^6Li spectra taken at several temperatures are shown in Figure 4. The racemate showed a single peak at 2.80 ppm assigned to the Li^+ on **7** as well as small amounts of solvated lithium ion¹⁸ at 0.5–1.0 ppm at all temperatures between -30 and $-80 \text{ }^\circ\text{C}$. A single lithium signal is consistent with the monomer, dimer-1, dimer-2, and polymer structures shown in Figure 3. In contrast, the enantioenriched compound showed

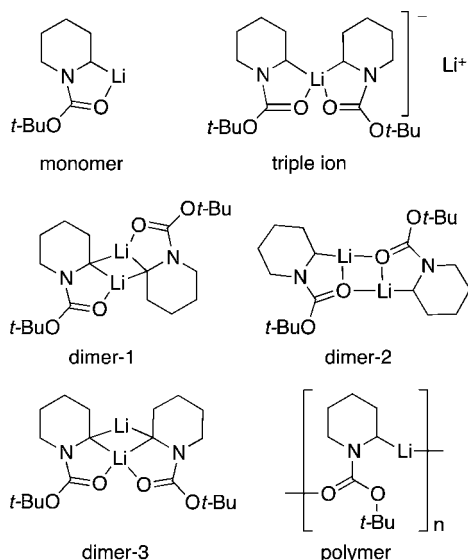


Figure 3. Possible solution structures for **7** (neglecting the absolute and relative configurations of the metal-bearing carbons).

an approximately 1:1 ratio of **7** and solvated Li^+ at $-80\text{ }^\circ\text{C}$ that changed as the temperature increased. The two lithium signals observed at $-80\text{ }^\circ\text{C}$ are consistent with the triple ion and dimer-3 structures. The growth of a shoulder on the upfield signal as the temperature was raised indicates a second type of solvated lithium ion, and the changes in line shape suggest a dynamic exchange process among solution species.

Partial ^{13}C spectra of *rac-7* and *S-7* (93:7 er) at $-81\text{ }^\circ\text{C}$ (Figure 5) showed a peak at 56.2 ppm that was split into a 1:1:1 triplet ($J = 11.9\text{ Hz}$) as a result of 1J coupling between ^6Li

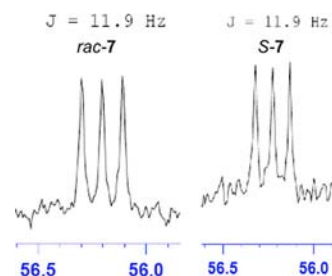


Figure 5. Partial ^{13}C spectra of (left) $\{^6\text{Li}\}$ -*rac-7* and (right) $\{^6\text{Li}\}$ -*S-7* (93:7 er) in TMEDA/ Et_2O at $-80\text{ }^\circ\text{C}$, showing the metal-bearing carbon at 56.2 ppm, referenced to external CD_3OD at 49.0 ppm.

and C-2 of a contact ion pair; at $-30\text{ }^\circ\text{C}$, this coupling was no longer evident, consistent with a solvent-separated ion pair. Being indicative of a single lithium in contact with the carbanionic carbon, this triplet rules out dimer-1 and dimer-3. The resonance of the carbonyl carbon appeared at 160.1 ppm for both *rac-7* and *S-7*. Thus, no difference between the chemical shifts of this peak for racemic and enriched **7** in TMEDA/ Et_2O could be detected, even though we took care to reference the spectra to the chemical shift of methanol- d_4 in a concentric capillary. These similarities suggest that the structure of the organolithium species being observed is the same whether the species is racemic or enantioenriched. It should be noted, however, that these observations do not preclude the presence of other organolithium species in the solution.

To summarize: for *rac-7*, the ^6Li and ^{13}C NMR data are consistent with the monomer, dimer-2, or polymer structure but not the triple ion, dimer-1, or dimer-3 structure. For *S-7*, the ^6Li spectrum is consistent with the triple ion or dimer-3 structure at $-80\text{ }^\circ\text{C}$, with other structures evident at

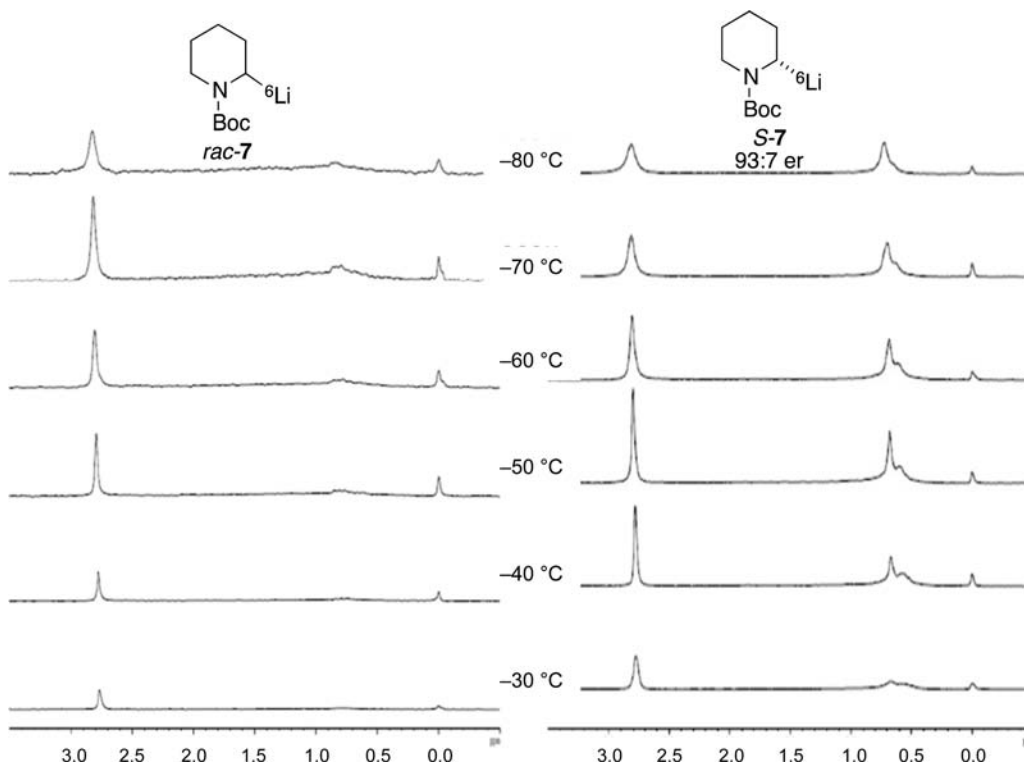


Figure 4. ^6Li NMR spectra of **7** obtained by transmetalation of **12** in Et_2O in the presence of 4 equiv of TMEDA: (left) $\{^6\text{Li}\}$ -*rac-7*; (right) enantioenriched $\{^6\text{Li}\}$ -*S-7*. The peaks at 0 ppm are external 1.0 M $^6\text{LiCl}$ in CD_3OD in a concentric capillary.

temperatures greater than or equal to $-60\text{ }^{\circ}\text{C}$. The coupling seen in the partial ^{13}C spectra are consistent with the monomer, triple ion, dimer-2, or polymer structures.

Attempts were made to monitor changes in the solution structure during a catalytic resolution. To that end, a mixture of racemic stannane **12**, TMEDA (4 equiv), and the conjugate acid of ligand **10** (10 mol %) was placed in an NMR tube and cooled to $-78\text{ }^{\circ}\text{C}$. A solution of $n\text{-Bu}^6\text{Li}$ was added, and the sample was transferred to an NMR probe cooled to $-80\text{ }^{\circ}\text{C}$. The temperature was maintained at $-80\text{ }^{\circ}\text{C}$ for 2 h to complete the tin–lithium exchange, then raised to $-45\text{ }^{\circ}\text{C}$ for 3 h to effect the dynamic resolution, and finally cooled back to $-80\text{ }^{\circ}\text{C}$ (we previously determined that enantioenriched **7** is configurationally stable at $-80\text{ }^{\circ}\text{C}$ ¹⁶). Four spectra were obtained, with an accumulation time of $\sim 1\text{ h}$ in each case (Figure 6). Most noticeably, the 1:1:1 triplet indicating a

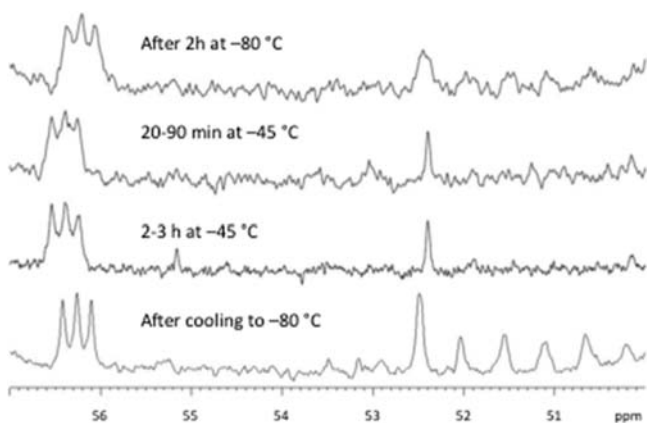


Figure 6. Partial ^{13}C spectra of a CDR of **7** conducted in an NMR tube.

contact ion pair comprising one carbon and one lithium atom is evident in all four spectra. Changes were also seen in the region between 50 and 53 ppm: a series of unassigned peaks are barely evident in the top spectrum, disappear in the spectra at $-45\text{ }^{\circ}\text{C}$, and become much more prominent at the end of the resolution. Quenching the solution in the NMR tube with phenyl isocyanate and subsequent workup afforded an 89:11 ratio of pipercolic acid anilide enantiomers [see the Supporting Information (SI) for details].^{17a}

X-ray Crystal Structure of Ligand 10. The dilithio ligand **10** formed beautiful crystals when an ether solution of the ligand was cooled in the absence of TMEDA. The ligand crystallized as an octamer formed by stacking of two cyclic tetramers on top of each other. Each tetramer features a 16-membered ring consisting of four $-\text{O}-\text{Li}-\text{NMe}-\text{Li}-$ units. Figure 7a shows a ball-and-stick structure, including two ethers of crystallization. Figure 7b is a ChemDraw rendering of one of the 16-membered tetramer rings, with one monomer highlighted in blue. It should be noted that for each monomer, one of the lithium atoms is chelated by two nitrogens and the oxygen, while the second lithium bridges the methylated nitrogen to the oxygen of the next monomer. Figure 7c shows the octamer, with the second tetramer rendered in red. There are two types of bridging between the two 16-membered rings: the methylated nitrogens in one tetramer are coordinated to the bridging lithiums of the other tetramer, while the chelated lithiums in one tetramer are coordinated to the oxygens in the other tetramer. This results in eight four-coordinate lithium atoms and eight 3-coordinate lithium atoms in the crystal. It is noteworthy that the eight *N*-methyl substituents of these chiral ligands completely fill the interior cavity of the octamer.

Configurational Stability of 7. In these studies, we chose to generate organolithium **7** by tin–lithium exchange from stannane **12** because we wanted to avoid the possibility of incomplete deprotonation of **6**, which could complicate the analysis of the product mixtures, and because we wished to generate **7** efficiently while also having evidence of its formation.

Scheme 6 summarizes the experiments used to evaluate the configurational stability of **7** formed by tin–lithium exchange in

Scheme 6. Transmetalation and Configurational Stability Studies

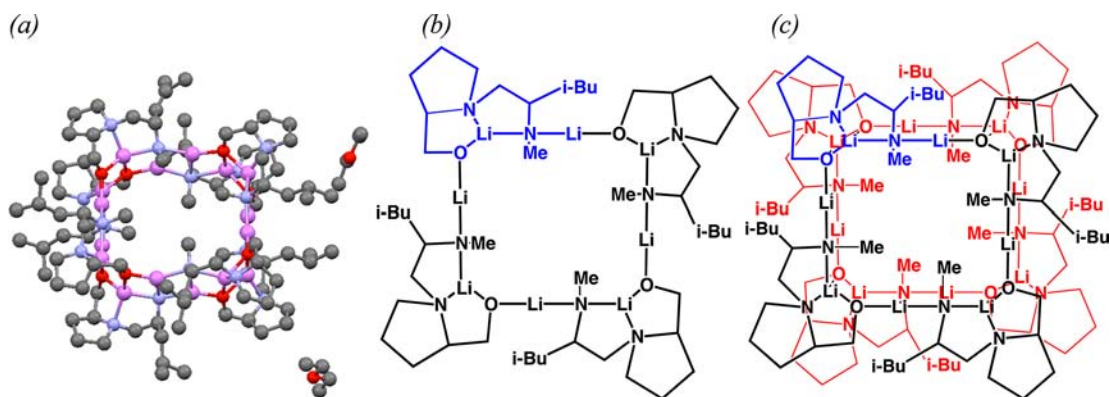
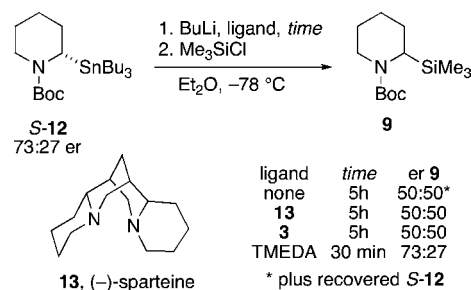


Figure 7. X-ray crystal structure of dilithio ligand **10**: (a) ball-and-stick rendering of the octameric crystal structure comprising two stacked 16-membered rings and two molecules of diethyl ether; (b) one 16-membered-ring tetramer, with one monomer colored blue; (c) stacked tetramers, with the rear tetramer colored red.

the absence or presence of (–)-sparteine (**13**), bispidine **3**, or TMEDA. We previously found that tin–lithium exchange of *S*-**12** in the absence of any ligand at temperatures of –60 °C or above result in racemic product.¹⁶ Below –60 °C, the lithiation is too slow to be synthetically useful, but it was attempted at –78 °C to investigate the configurational stability in the absence of ligands. At this temperature, the half-life for tin–lithium exchange is >5 h (see the SI for kinetic details). After treatment of **12** with *n*-BuLi for 5 h at –78 °C, quenching with Me₃SiCl produced a mixture of **12** and **9**, but the latter was racemic. In the presence of either **13** or **3**, TLC monitoring showed that transmetalation of *S*-**12** (73:27 er) to give **7** was complete after 5 h; however, quenching with Me₃SiCl afforded racemic **9**. This result is in contrast to the 87:13 er of **7** obtained by deprotonation using *sec*-BuLi in the presence of **13**,^{3a} perhaps reflecting different mechanisms for the formation of **7** involving different types of lithium ligation in different solvents or in the presence of different amines. In tetrahydrofuran in the absence of diamines, for example, tin–lithium exchange occurs with complete retention of configuration.^{4a} As noted previously,¹⁶ TMEDA plays a unique role in the racemization and DTR of lithiopiperidine **7**: both processes are first order in [TMEDA] when 0–1 molar equiv of TMEDA is used. After treatment of stannane **12** (73:27 er) with *n*-BuLi for only 30 min at –78 °C in the presence of 1 equiv of TMEDA, quenching with Me₃SiCl revealed complete transmetalation, and **9** was obtained in 73:27 er. Of the ligands tested, only TMEDA is suitable for the CDR of **7** following tin–lithium exchange, consistent with its previously-noted uniqueness.¹⁶

DTR Kinetics at –55 °C. Previously, the barriers for inversion in the DTR of *rac*-**7** by stoichiometric quantities of **8** were determined at four temperatures ranging from –10 to +20 °C.¹⁶ Because we planned to investigate catalytic resolution at considerably lower temperatures, we decided to measure the kinetics of stoichiometric DTR at –55 °C. The time evolution of the stoichiometric DTR of *rac*-**7** by **8** in the presence of 1.2 equiv of TMEDA was measured, as illustrated in Figure 8. The evolution of the major enantiomer (in this case, the *S* enantiomer) is given by the equation

$$[S]_t = [S]_{\text{eq}} + ([S]_0 - [S]_{\text{eq}}) e^{-k_{\text{obs}}t} \quad (1)$$

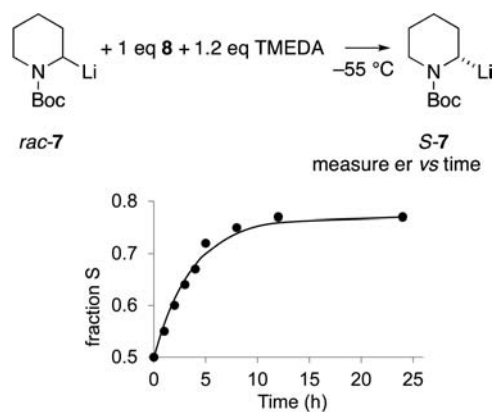


Figure 8. Evolution of the fraction of the *S* enantiomer in the stoichiometric DTR of **7** by **8** (1.0 equiv) in the presence of TMEDA (1.2 equiv) at –55 °C. A nonlinear least-squares fit of the data to eq 1 using $[S]_{\text{eq}} = 0.77$ and $[S]_0 = 0.5$ yielded $k_{\text{obs}} = (7.48 \pm 0.63) \times 10^{-5} \text{ s}^{-1}$.

where $[S]_t$ is the fraction of the *S* enantiomer at time t and $[S]_0$ and $[S]_{\text{eq}}$ are the fractions of the *S* enantiomer at $t = 0$ and $t = \infty$, respectively, at the temperature of interest (here, $[S]_0 = 0.5$ and $[S]_{\text{eq}} = 0.77$). The data revealed a half-life of ~3 h at this temperature.

The Effect of [8] on the Dynamic Resolution of 7. To evaluate how varying the amount of chiral ligand **8** affects the dynamic resolution, experiments were conducted using catalysts loadings of 15, 20, 50, 80, and 100 mol %. After 5 h at –55 °C, er values of 63:37, 66:34, 71:29, 75:25, and 78:22 were observed for **9** (Figure 9, diamonds). The data in Figure 9

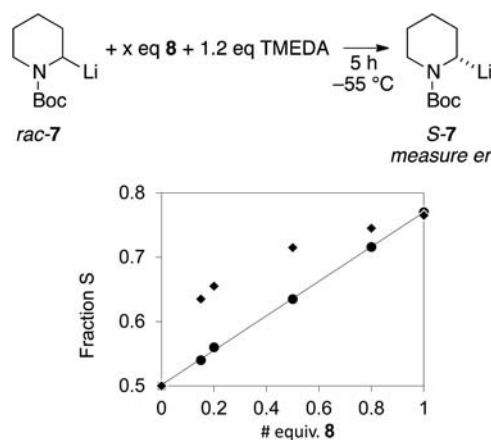


Figure 9. Effect of varying [8] on the dynamic resolution of *rac*-**7** with TMEDA (1.2 equiv) at –55 °C in ether for 5 h, after quenching with Me₃SiCl. The circles and the straight line indicate the fractions calculated if the system were to contain *rac*-**7**–TMEDA and **7**·**8** with an er of 77:23. The diamonds indicate the experimental values observed after 5 h.

clearly show that catalysis occurred, since the observed er is always higher than what would have been predicted if **7** not bound to **8** was racemic (Figure 9, circles), as was realized at higher temperatures (see Figure 15, below). This is all the more surprising since the values should be lower than the predicted value if equilibrium were not yet reached. The SI contains a similar plot for ligand **10**. Thus, a quantitative evaluation of the rates of resolution with differing amounts of **8** and **10** was undertaken.

The dependence of the rate of resolution of lithiopiperidine **7** on chiral ligands **8** and **10** was investigated at –20 °C in the presence of TMEDA (1.0 equiv) in Et₂O (see the SI for details). Figure 10 shows plots of the observed first-order rate constant versus the amount of **8** or **10** over the range 0–1 equiv. A nonlinear fit of the data to the equation $k_{\text{obs}} = k[L^*]^n$ afforded $n = 0.5$ and $k = (1.59 \pm 0.06) \times 10^{-3} \text{ M}^{-0.5} \text{ s}^{-1}$ for **8**. A similar fit of the observed rate constants plotted against [10] revealed $n = 0.265 \pm 0.022$ and $k = (9.49 \pm 0.12) \times 10^{-4} \text{ M}^{-0.265} \text{ s}^{-1}$ (see the SI for details). Thus, the reaction is half order in [8] and approximately one-fourth order in [10]. A fractional order is indicative of a mechanism involving deaggregation of the chiral ligand.

The Effect of [TMEDA] on CDR of 7. As noted above, TMEDA plays a unique role in the inversion dynamics of lithiopiperidine **7** (both enantiomerization and DTR).¹⁶ It was therefore of interest to explore the kinetic role of TMEDA in the CDR of **7**. The time evolution of *S*-**7** under CDR conditions in the presence of varying amounts of TMEDA (0–4 equiv) was followed, and the rate constants were measured

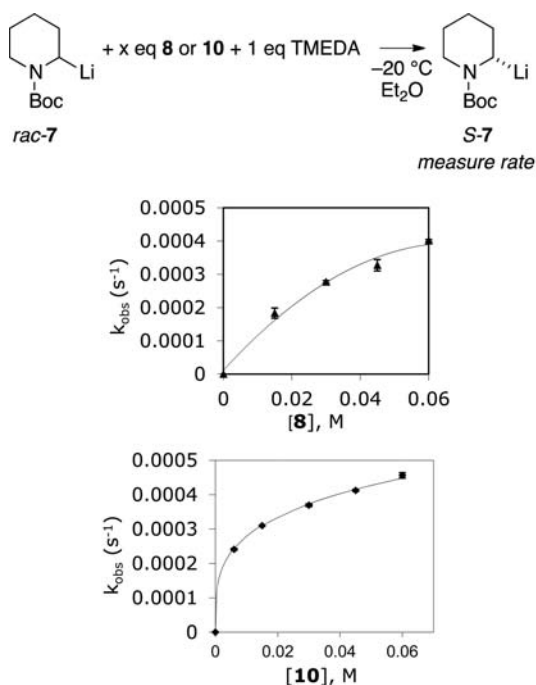


Figure 10. Plots of the observed rate constant k_{obs} vs the concentrations of (top) **8** and (bottom) **10** for the dynamic resolution of *rac*-**7** (0.06 M) in the presence of TMEDA (1.0 equiv) at $-20\text{ }^{\circ}\text{C}$ in Et_2O . The point at the origin in each graph is not experimental.

(Figure 11). Upward curvature is emblematic of a higher-order dependence of the rate on [TMEDA]. A nonlinear parametric

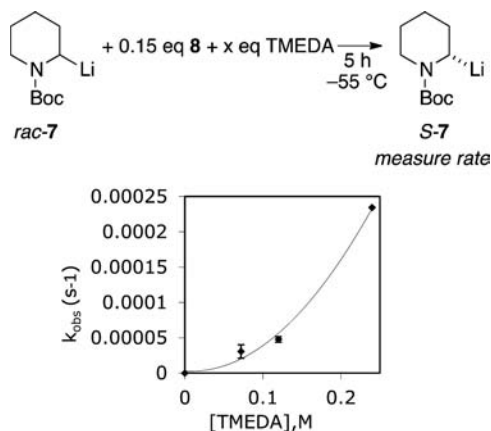


Figure 11. Effect of varying [TMEDA] on the CDR of **7** (0.06 M) in the presence of **8** (0.15 equiv) in ether at $-55\text{ }^{\circ}\text{C}$ for 4 h. The solid curve is a fit to the equation $k_{\text{obs}} = k[\text{TMEDA}]^n$ with $k = (4.02 \pm 0.11) \times 10^{-3} \text{ M}^{-2} \text{ s}^{-1}$ and $n = 1.99$.

fit of the equation $k_{\text{obs}} = k[\text{TMEDA}]^n$ revealed a second-order dependence on [TMEDA], with $n = 1.99$ and $k = (4.02 \pm 0.11) \times 10^{-3} \text{ M}^{-2} \text{ s}^{-1}$. This indicates that the transition structure of the rate-limiting step in the CDR contains two TMEDA molecules.

Racemization of 7 with Excess TMEDA. Since the dynamics of racemization of *S*-**7** were previously determined in the presence of 1 equiv of TMEDA, and since we observed a second-order dependence of the CDR on [TMEDA], we re-examined the racemization kinetics, this time in the presence of excess TMEDA. The enantiomerization was followed by

generating organolithium **7** (er 85:15 or 96:4 *S*:*R*) using tin–lithium exchange in Et_2O at $-78\text{ }^{\circ}\text{C}$ with BuLi and 2 or 4 equiv of TMEDA, warming the reaction mixture to the desired temperature for different time periods, and then cooling to $-78\text{ }^{\circ}\text{C}$ and quenching with excess Me_3SiCl as previously described (see the SI for details).¹⁶ The rate constants were determined by nonlinear fits to the zero-order plots. Eyring analysis of the rate constants at their respective temperatures in the presence of varying amounts of TMEDA provided the thermodynamic parameters listed in Table 1. The plots of Gibbs free energy as a

Table 1. Thermodynamic Parameters for Racemization of **7** with Varying Amounts of TMEDA

entry	RLi-L	equiv of TMEDA	ΔH^\ddagger (kcal/mol)	ΔS^\ddagger ($\text{cal mol}^{-1} \text{ K}^{-1}$)
1 ^a	7·TMEDA	1.0	18.1 ± 0.7	5.0 ± 3.2
2	7·TMEDA	2.0	20.1 ± 1.8	9.9 ± 7.6
3	7·TMEDA	4.0	22.5 ± 2.0	16.7 ± 8.8

^aData taken from ref 14.

function of temperature¹¹ for various amounts of TMEDA (Figure 12a) reveal that racemization has a significantly higher energy barrier with 4 equiv of TMEDA than with 1 or 2 equiv at all temperatures between -80 and $0\text{ }^{\circ}\text{C}$. Figure 12b shows that in the presence of 2 equiv of TMEDA, racemization and resolution of **7** by stoichiometric amounts of **8** have equal free energy barriers at $-33\text{ }^{\circ}\text{C}$.¹¹ Below that temperature, resolution has a lower barrier.

In a preliminary communication, we showed that the rate of enantiomerization of **7** is first order in TMEDA up to 1 equiv.¹⁶ However, the above experiments revealed that the barrier for enantiomerization is raised significantly in the presence of excess TMEDA. Because our CDR studies were carried out using excess TMEDA, we decided to study the rate of enantiomerization with excess TMEDA. The details are given in the SI, and the results are plotted in Figure 13. There is an inverse dependence of the racemization rate on [TMEDA] when TMEDA is in excess relative to **7**. Thus, for the purposes of developing the CDR, 2–4 equiv of TMEDA beneficially retards racemization. In the preparative experiments described later and also those using ligands **10** and **11**,¹⁷ we employed 4 equiv of TMEDA, which served to accelerate resolution and retard racemization.

Approach to the $-55\text{ }^{\circ}\text{C}$ Equilibrium from Either Direction. The zero-order plots for the CDR starting from *rac*-**7** approach but never exceed the er value observed in the stoichiometric DTR (77:23). In our study of the CDR of *N*-(trimethylallyl)pyrrolidine **2**, we showed that *R*-**2** (93:7 er) maintained configurational stability under the catalytic conditions for 90 min.⁹ For lithiopiperidine **7**, we employed stannylpiperidine *S*-**12** with 96:4 er,^{17a} and it was of interest to see whether this er would be maintained under the catalytic conditions or drop to the 77:23 er observed when starting with racemate. We subjected both enantiomers to catalytic conditions (15 mol % **8**, 2 equiv of TMEDA, $-55\text{ }^{\circ}\text{C}$) and recorded the evolution of the er, as shown in Figure 14. In both experiments, the final er matched the er in the stoichiometric DTR. The rate constant k_{SR} for equilibration of *S*-**7** (96:4 er) in the presence of 2 equiv of TMEDA and 15 mol % **8** is $(1.93 \pm 0.11) \times 10^{-5} \text{ s}^{-1}$. Similarly, the rate constant k_{RS} for CDR of *R*-**7** (72:28 er) is $(6.24 \pm 0.45) \times 10^{-5} \text{ s}^{-1}$. The $k_{\text{RS}}/k_{\text{SR}}$ ratio is

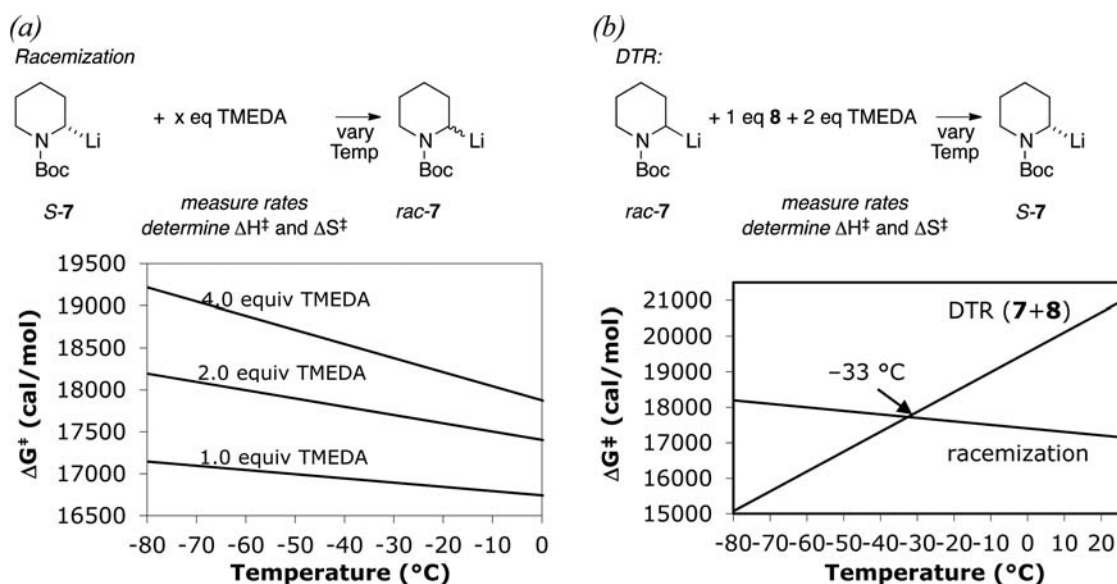


Figure 12. (a) Plots of ΔG^\ddagger vs temperature for the enantiomerization of **7** with varying amounts of TMEDA. (b) Plots of ΔG^\ddagger vs temperature for racemization and stoichiometric DTR of **7** in the presence of 2 equiv of TMEDA.¹¹

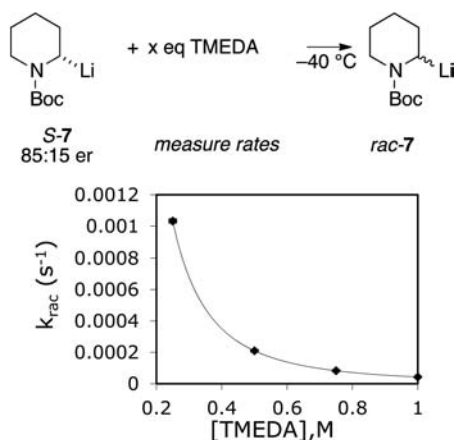


Figure 13. Effect of 1–4 equiv of TMEDA on the rate of racemization of **7** (0.25 M) at -40°C .

3.23, which is similar to the *S*-**7**·**8**/*R*-**7**·**8** ratio in a DTR (3.35 for **77**:**23** er).

Effect of Temperature on the Position of the Equilibrium. The above discussion emphasizes the importance of staying below the crossover temperature to ensure that the free energy barrier for resolution is below the barrier for racemization. Two control experiments demonstrated the importance of temperature control. Racemic lithiopiperidine **7** was subjected to catalytic conditions (4 equiv of TMEDA and 15 mol % **8** or **10** at -55°C), and the er was measured at several time intervals until it reached 76:24 for **8** and 95:5 for **10**. The temperature was then raised to 0°C , and the er was monitored again. The dramatic results are illustrated in Figure 15. At 0°C , the er dropped dramatically to \sim 55:45. Clearly, careful control of the temperature is necessary to achieve a CDR.

Optimized Conditions for CDR. Given the above findings, we decided on the optimum conditions of 5–15 mol % **10** and 4 equiv of TMEDA, which we subsequently used in several

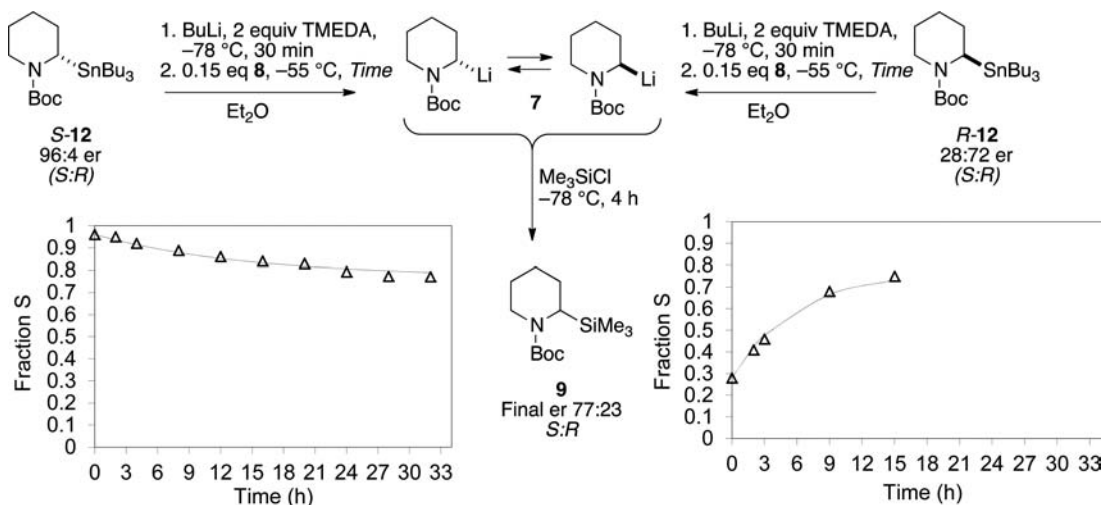


Figure 14. Evolution of CDR starting from enantioenriched *R*- or *S*-**12**.

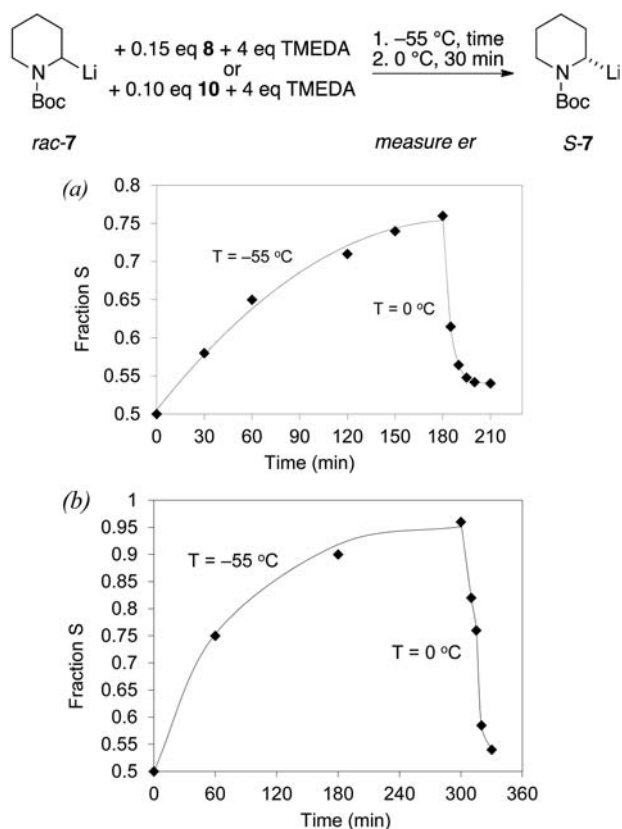


Figure 15. Proof of a low-temperature process that effects a catalytic resolution at $-55\text{ }^{\circ}\text{C}$ but which at $0\text{ }^{\circ}\text{C}$: CDR of 7 in the presence of TMEDA (4.0 equiv) at $-55\text{ }^{\circ}\text{C}$ followed by warming to $0\text{ }^{\circ}\text{C}$ for 30 min results in rapid racemization using either (a) ligand 8 or (b) ligand 10.

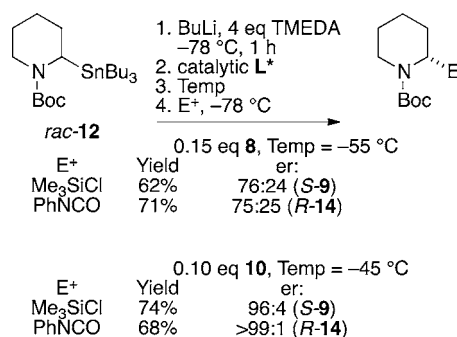
synthetic applications. Both direct electrophilic substitutions and transmetalations with ZnCl_2 followed by Cu(I) or Pd(0) cross-couplings were demonstrated by numerous examples with a high degree of enantioselectivity, usually $\geq 95:5$ er.¹⁷ Examples using trimethylsilyl chloride and phenyl isocyanate as electrophiles are given in Scheme 7 for comparison of ligands 8 and 10.

SUMMARY AND CONCLUSIONS

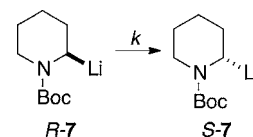
Several important details have emerged from these studies:

1. NMR data are inconclusive as to the solution structure of 7, although differences in the ^6Li spectra of *rac*-7 and *S*-7 are evident.

Scheme 7. Optimized CDR Conditions



2. The ^6Li spectra of *S*-7 exhibit dynamic phenomena as the temperature is raised to $-60\text{ }^{\circ}\text{C}$ and above.
3. Splitting of the ^{13}C NMR signal for the carbanionic carbon persists throughout the CDR. Other signals appear in the same region, suggesting the presence of other species.
4. Consistent with faster organolithium dynamics at higher temperatures, rapid racemization is observed when the temperature of the reaction mixture containing resolved 7 is raised to $0\text{ }^{\circ}\text{C}$.
5. Chiral ligands 8 and 10 increase the rate of CDR. The kinetic order for CDR of lithiopiperidine 7 is 0.5 for 8 and 0.265 for 10. Fractional orders implicate deaggregation of the chiral catalysts. Ligand 10 is an octamer in the solid state.
6. Excess TMEDA accelerates the CDR. Although the stoichiometric DTR is first order in $[\text{TMEDA}]$,¹⁶ the CDR (0.15 equiv of 8) is second order in $[\text{TMEDA}]$.
7. Excess TMEDA retards racemization. The rate constant for enantiomerization of lithiopiperidine 7 is at a maximum when the ratio 7:TMEDA = 1. Racemization is first order in $[\text{TMEDA}]$ up to 1 equiv of TMEDA (however, racemization is very fast in the absence of TMEDA) and inverse order when excess TMEDA is present (up to 4 equiv).
8. The final er values of the stoichiometric DTR and the CDR are the same.
9. Temperature control is critical to the success of the CDR.



10. For the CDR that converts *R*-7 to *S*-7 using L^* as the catalyst, the rate law is

$$\frac{d[\text{S-7}]}{dt} = k[\text{R-7}][\text{TMEDA}]^2[\text{L}^*]^n$$

where $n = 0.5$ for 8 and 0.265 for 10.

We have observed CDR for five combinations of the organolithium species, catalyst, and achiral ligand (Figure 16): 2-lithio-*N*-(trimethylallyl)pyrrolidine 2 as the organolithium with either lithium diaminoalkoxide 4 or (–)-sparteine as the catalyst and *N,N'*-diisopropylbispidine 3 as the achiral ligand⁹ and 2-lithio-*N*-Boc-piperidine 7 as the organolithium with either lithium diaminoalkoxide 8 or dilithio ligands 10 or 11 as the catalyst and TMEDA as the achiral ligand.¹⁷ What is clear from these studies is that ligand exchange is an important process in dynamic resolutions of 7 and 2 both stoichiometric and catalytic conditions. The effect of a ligand on the rate of carbanion inversion of a chiral organolithium species can change with the ligand/organolithium molar ratio. It is also clear that an achiral ligand and careful control of temperature are necessary to achieve a catalytic resolution. As a guide for choosing the temperature, we used the “crossover temperature”, where the free energy barrier for racemization and dynamic resolution are equal: below this temperature, CDR can occur, but above this temperature it cannot. Further refinement of the temperature is based on the free energy barrier for the CDR such that a reasonable half-life can be achieved.

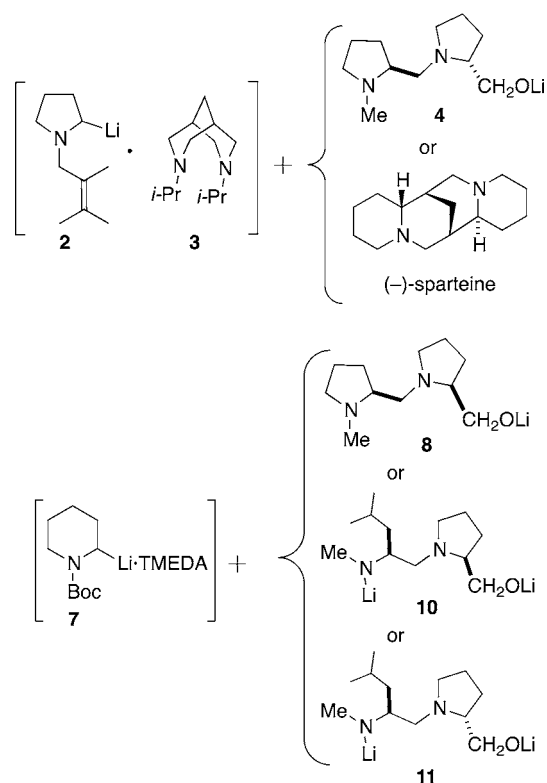


Figure 16. Organolithium and ligand combinations amenable to CDR.

If the organolithium species and the chiral ligand are monomeric, CDR is not possible because the process would violate the principle of microscopic reversibility. However, as shown by Toru and co-workers,⁶ irreversible population of a homochiral aggregate from a racemic monomer or a heterochiral aggregate by CDR is possible. In the case of the piperidines studied in this work, there is some evidence of differences between the solution structures of racemic and enantioenriched **7**. In this system, we found no visible evidence of aggregate precipitation but did see evidence of variable solution structure that is dependent on temperature. Furthermore, we also observed a change in the final enantiomer ratio that is dependent on temperature. In addition, the fractional order of the CDR with respect to L^* provides clear evidence that deaggregation of the resolving ligand is operative in the dynamic resolution of **7**. We have also demonstrated that the catalytic resolution requires exchange with an achiral ligand, in this case TMEDA.¹⁹ These observations may be due to a change in solution structure between racemic and enantioenriched **7**, such as the formation of a homochiral aggregate at low temperature. At higher temperatures such as 0 °C, new pathways for racemization become operative, such that the organolithium that is presumably complexed to TMEDA racemizes rapidly while the remainder, complexed to L^* , remains enantioenriched. Additionally, the fractional kinetic order in ligands **8** and **10** implicates changes in the aggregation state of the resolving ligand in the rate-determining step. Our working hypothesis of this phenomenon is that a successful CDR depends on ligand exchange with an achiral ligand and on aggregation–deaggregation phenomena of the species in solution, including the chiral organolithium and/or the resolving ligand.

EXPERIMENTAL SECTION

For general experimental conditions, see the SI.

General Procedure for Determining the Effect of Varying [8] on Dynamic Resolution of 7 in the Presence of TMEDA. In oven-dried tubes equipped with stir bars and capped with rubber septa, *rac*-**12** (0.06 M in ether) was treated with BuLi (1.2 equiv) and TMEDA (1.2 equiv) at –78 °C for 1 h under argon to effect tin–lithium exchange, affording *rac*-**7**-TMEDA. The concentration of **8** was varied (0.0 to 100 mol %), and the tubes were quickly transferred to the –55 °C bath. After 5 h at this temperature, the tubes were transferred to the –78 °C bath and rapidly quenched with excess Me₃SiCl. The silanes were subsequently analyzed by chiral-stationary-phase supercritical fluid chromatography (CSP-SFC) with monitoring at 210 nm. See the SI for details.

Activation Parameters for Racemization of 7 with 2.0 equiv of TMEDA. In a typical kinetic run, *S*-**12** (85:15 er, 0.06 M in ether) in the presence of TMEDA (2.0 equiv) was treated with BuLi (1.2 equiv) at –78 °C for 30 min under nitrogen in oven-dried septum-capped tubes equipped with a stir bars to effect tin–lithium exchange. The tubes were quickly transferred to a second thermostatted bath and warmed to the desired temperature. At various time intervals a tube was cooled to –78 °C and rapidly quenched with excess Me₃SiCl. After 4 h, MeOH (2 mL) was added, and the mixture was extracted into Et₂O. The silanes were subsequently analyzed by CSP-SFC with monitoring at 210 nm. The rate constants were determined by nonlinear fits to the zero-order plots, and Eyring analysis of the temperature-dependent rate constants provided the thermodynamic parameters. See the SI for details.

Details of X-ray Crystal Structure Determination of Ligand 10. A clear, colorless chunklike specimen of C₉₆H₁₉₂Li₁₆N₁₆O₈·(C₄H₁₀O)₂ (approximate dimensions 0.280 mm × 0.300 mm × 0.340 mm) was used for the X-ray crystallographic analysis. The X-ray intensity data were measured on a Bruker Apex 1K diffractometer. Integration of the data using a triclinic unit cell yielded a total of 21 236 reflections to a maximum θ angle of 26.48° (0.80 Å resolution), of which 18 549 were independent (average redundancy = 1.145, completeness = 83.5%, $R_{\text{int}} = 3.81\%$, $R_{\text{sig}} = 7.20\%$) and 14 814 (79.86%) were greater than $2\sigma(F^2)$. The final cell constants were determined to be $a = 11.668(4)$ Å, $b = 17.093(6)$ Å, $c = 18.174(6)$ Å, $\alpha = 64.950(5)^\circ$, $\beta = 76.278(5)^\circ$, $\gamma = 88.581(6)^\circ$, and $V = 3178.2(19)$ Å³ on the basis of refinement of the XYZ-centroids of reflections above $20\sigma(I)$. Data were corrected for absorption effects using the multiscan method (SADABS). The ratio of minimum to maximum apparent transmission was 0.534–0.711.

The structure was solved and refined using the Bruker SHELXTL software package in the space group $P1$ with $Z = 1$ for the formula unit C₁₀₄H₂₁₂Li₁₆N₁₆O₁₀. The final anisotropic full-matrix least-squares refinement on F^2 with 1343 variables converged at $R_1 = 7.53\%$ for the observed data and $wR_2 = 22.77\%$ for all data. The goodness of fit was 1.036. The largest peak in the final difference electron density synthesis was 0.869 e/Å³, and the largest hole was –0.564 e/Å³, with a root-mean-square deviation of 0.076 e/Å³. On the basis of the final model, the calculated density was 1.023 g/cm³ and $F(000)$ was 1076e.

ASSOCIATED CONTENT

Supporting Information

Full experimental details, including kinetic plots, data analysis, and the NMR experiments. This material is available free of charge via the Internet at <http://pubs.acs.org>.

AUTHOR INFORMATION

Corresponding Author

bgawley@uark.edu

Notes

The authors declare no competing financial interest.

ACKNOWLEDGMENTS

We thank the National Science Foundation (CHE 0616352 and 1011788) and the Arkansas Biosciences Institute for direct support of this work. T.P. thanks the NSF-REU Program for a summer fellowship (CHE 0851505). Core facilities were funded by the Arkansas Biosciences Institute and the National Institutes of Health (P30 RR031154 and P30 GM103450). We also thank Professors Donna Blackmond, Iain Coldham, David Collum, and Jonathan Clayden for helpful discussions.

REFERENCES

- (1) (a) Clayden, J. *Organolithiums: Selectivity for Synthesis*; Pergamon Press: London, 2002. (b) *Organolithiums in Enantioselective Synthesis*; Hodgson, D. M., Ed.; Springer: Berlin, 2003; Vol. 5. (c) *The Chemistry of Organolithium Compounds*; Rappoport, Z., Marek, I., Eds.; Wiley: Chichester, 2004. (d) *Organometallics: Compounds of Group 1 (Li ... Cs)*; Majewski, M., Snieckus, V., Eds.; Thieme: Stuttgart, 2006; Vol. 8a. (e) *Stereochemical Aspects of Organolithium Compounds*; Gawley, R. E., Ed.; Topics in Stereochemistry, Vol. 26; Wiley-VCH: Weinheim, Germany, 2010.
- (2) (a) Hoppe, D.; Hense, T. *Angew. Chem., Int. Ed. Engl.* **1997**, *36*, 2283–2316. (b) Hoppe, D.; Christoph, G. In *The Chemistry of Organolithium Compounds*; Rappoport, Z., Marek, I., Eds.; Wiley: Chichester, 2004; pp 1055–1164. (c) Beak, P.; Johnson, T. A.; Kim, D. D.; Lim, S. H. *Top. Organomet. Chem.* **2003**, *5*, 139–176. (d) Kizirian, J.-C. *Top. Stereochem.* **2010**, *26*, 189–251. (e) Mitchell, E. A.; Peschiulli, A.; Lefevre, N.; Meerpoel, L.; Maes, B. U. W. *Chem.—Eur. J.* **2012**, *18*, 10092–10142.
- (3) (a) Bailey, W. F.; Beak, P.; Kerrick, S. T.; Ma, S.; Wiberg, K. B. *J. Am. Chem. Soc.* **2002**, *124*, 1889–1896. (b) Coldham, I.; O'Brien, P.; Patel, J. J.; Raimbault, S.; Sanderson, A. J.; Stead, D.; Whittaker, D. T. E. *Tetrahedron: Asymmetry* **2007**, *18*, 2113–2119. (c) Metallinos, C.; Dudding, T.; Zaifman, J.; Chaytor, J. L.; Taylor, N. J. *J. Org. Chem.* **2007**, *72*, 957–963.
- (4) (a) Stead, D.; Carbone, G.; O'Brien, P.; Campos, K. R.; Coldham, I.; Sanderson, A. *J. Am. Chem. Soc.* **2010**, *132*, 7260–7261. (b) Dixon, A. J.; McGrath, M. J.; O'Brien, P. In *Organic Syntheses*; Wiley: New York, 2009; Collect. Vol. 11, pp 25–37.
- (5) (a) Beak, P.; Anderson, D. R.; Curtis, M. D.; Laumer, J. M.; Pippel, D. J.; Weisenburger, G. A. *Acc. Chem. Res.* **2000**, *33*, 715–727. (b) Coldham, I.; Dufour, S.; Haxell, T. F. N.; Howard, S.; Vennall, G. P. *Angew. Chem., Int. Ed.* **2002**, *41*, 3887–3889. (c) Coldham, I.; Dufour, S.; Haxell, T. F. N.; Vennall, G. P. *Tetrahedron* **2005**, *61*, 3205–3220. (d) Whisler, M. C.; MacNeil, S.; Snieckus, V.; Beak, P. *Angew. Chem., Int. Ed.* **2004**, *43*, 2206–2225. (e) Coldham, I.; Dufour, S.; Haxell, T. F. N.; Patel, J. J.; Sanchez-Jimenez, G. *J. Am. Chem. Soc.* **2006**, *128*, 10943–10951. (f) Coldham, I.; Raimbault, S.; Chovatia, P. T.; Patel, J. J.; Leonori, D.; Sheikh, N. S.; Whittaker, D. T. E. *Chem. Commun.* **2008**, 4174–4176. (g) Coldham, I.; Sheikh, N. S. *Top. Stereochem.* **2010**, *26*, 253–293. (h) Coldham, I.; Raimbault, S.; Whittaker, D. T. E.; Chovatia, P. T.; Leonori, D.; Patel, J. J.; Sheikh, N. S. *Chem.—Eur. J.* **2010**, *16*, 4082–4090.
- (6) (a) Nakamura, S.; Hirata, N.; Kita, T.; Yamada, R.; Nakane, D.; Shibata, N.; Toru, T. *Angew. Chem., Int. Ed.* **2007**, *46*, 7648–7650. (b) Nakamura, S.; Hirata, N.; Yamada, R.; Kita, T.; Shibata, N.; Toru, T. *Chem.—Eur. J.* **2008**, *14*, 5519–5527.
- (7) Bispidine 3 was first used as an exchangeable achiral ligand in catalytic deprotonations. See: McGrath, M. J.; O'Brien, P. *J. Am. Chem. Soc.* **2005**, *127*, 16378–16379.
- (8) If retentive substitution is assumed, this implies accumulation of the R organolithium.
- (9) Beng, T. K.; Yousaf, T. I.; Coldham, I.; Gawley, R. E. *J. Am. Chem. Soc.* **2009**, *131*, 6908–6909.
- (10) Tin–lithium exchange was used to generate 2 from 1, a process that fails in the absence of a diamine ligand.
- (11) In all cases, the best fits of the kinetic data were to reversible first-order plots.
- (12) Plots of ΔG^\ddagger vs temperature over a large temperature range assume that ΔH^\ddagger and ΔS^\ddagger are constant over the entire temperature range. Since the data in our Eyring plots were obtained over a small temperature range of 20–30 °C, the obtained values of ΔH^\ddagger and ΔS^\ddagger are valid over the temperature range where the measurements were made, and we assume that they offer a first approximation over the larger range.
- (13) Lee, W. K.; Park, Y. S.; Beak, P. *Acc. Chem. Res.* **2009**, *42*, 224–234.
- (14) (a) Low, E.; Gawley, R. E. *J. Am. Chem. Soc.* **2000**, *122*, 9562–9563. (b) Gawley, R. E.; Klein, R.; Ashweek, N. J.; Coldham, I. *Tetrahedron* **2005**, *61*, 3271–3280.
- (15) Barker, G.; O'Brien, P.; Campos, K. R. *ARKIVOC* **2011**, No. v, 217–229.
- (16) Coldham, I.; Leonori, D.; Beng, T. K.; Gawley, R. E. *Chem. Commun.* **2009**, 5239–5240; Corrigendum with correct enthalpy and entropy values: **2010**, 9267–9268.
- (17) (a) Beng, T. K.; Gawley, R. E. *J. Am. Chem. Soc.* **2010**, *132*, 12216–12217. (b) Beng, T. K.; Gawley, R. E. *Org. Lett.* **2011**, *13*, 394–397. (c) Beng, T. K.; Gawley, R. E. *Heterocycles* **2012**, *84*, 697–718.
- (18) Reich, H. J.; Sikorski, W. H.; Gudmundsson, B. Ö.; Dykstra, R. R. *J. Am. Chem. Soc.* **1998**, *120*, 4035–4036.
- (19) In the catalytic resolution of 2 by 4, the achiral ligand required is bispidine 3 (see ref 9).